INSTITUT DE FRANCE
Académie des sciences

Comptes Rendus

Mécanique

Ludovic Pauchard

Morphogenetic processes: from leaves to embryos

Volume 348, issue 6-7 (2020), p. 637-648

Published online: 16 November 2020
Issue date: 16 November 2020

https://doi.org/10.5802/crmeca.33

Part of Special Issue: Tribute to an exemplary man: Yves Couder

Guest editors: Martine Ben Amar (Paris Sciences & Lettres, LPENS, Paris, France), Laurent Limat (Paris-Diderot University, CNRS, MSC, Paris, France), Olivier Pouliquen (Aix-Marseille Université, CNRS, IUSTI, Marseille, France) and Emmanuel Villermaux (Aix-Marseille Université, CNRS, Centrale Marseille, IRPHE, Marseille, France)

Les Comptes Rendus. Mécanique *sont membres du Centre Mersenne pour l'édition scientifique ouverte*
www.centre-mersenne.org
e-ISSN : 1873-7234

Comptes Rendus
Mécanique
2020, 348, nº 6-7, p. 637-648
https://doi.org/10.5802/crmeca.33

Tribute to an exemplary man: Yves Couder

Morphogenesis, elasticity

Morphogenetic processes: from leaves to embryos

Ludovic Pauchard [a]

[a] Laboratoire FAST, Univ. Paris-Sud, CNRS, Université Paris-Saclay, F-91405 Orsay, France
E-mail: ludovic.pauchard@u-psud.fr

Abstract. The present manuscript is devoted to two works related to the spontaneous formation of patterns in Nature: venation in leaves and evolution of embryos. Morphogenetic processes and growth-induced instability phenomena are modelled through analogue experiments. The organization of veins in leaves is similar to what is expected from growth in a tensorial stress field that governs the formation of fractures, while the change in the shape of embryos is related to the deformation of a shell-like membrane whose properties evolve with time. The approaches resulting from analogue experiments is a way to explore specific properties of the media at a macroscopic scale. Thus the manuscript aims to focus on the analogue experiments, their adaptability to reproduce specific patterns and the relation between both growth-induced instability and mechanical behaviour of the matter.

Keywords. Morphology, Instability, Crack, Buckling, Drying.

2020 Mathematics Subject Classification. 00-01, 99-00.

Notes. Fully documented templates are available in the elsarticle package on CTAN.
Since 1880.

1. Introduction

Morphogenetic processes result in the spontaneous formation of patterns in Nature, providing various types of breaking the symmetry of initially homogeneous systems. In this way different physical, chemical or biological processes usually lead to the formation of similar patterns when they can be reduced to a similar mathematical structure [1]. Within this framework, the present manuscript aims to report two particular works initiated by Yves Couder: leaf venations and the shape change of an embryo during its evolution. The leaf venation is an optimal transportation network to distribute water and nutrients, and to collect the products of photosynthesis. Besides, the high-density network of veins also exhibits a mechanical resilience of the leave unrelated to transport [2]. Hence, the venation exhibits a large variety of morphologies whose particular characteristic is to form closed loops, e.g. the merging of two veins, in the event of damage to any vein. This characteristic belongs to the class of universality of the growth in a tensorial field contrarily to the growth in a scalar field as often thought. In particular, recent work beyond the scope

of the present manuscript has shown that vein growth and patterns are coordinated through the differences in mechanical properties between cell types [3]. The first study aimed to demonstrate that these morphologies correspond to what is expected from growth in a tensorial stress field such as the mechanical stress that governs the propagation of fractures in solids [4–6]. The second morphogenetic process reported here is involved during the evolution of embryos: during a specific stage, the mechanical behaviour of embryos is related to the deformation of a shell-like membrane. The study particularly aimed to highlight that the macroscopic deformation of the embryonic membrane is correlated to the local evolution of both its thickness and its mechanical properties [7].

In both works, the targeted approaches were investigated by focusing on analogue experiments intended to reproduce similar patterns. The following modelled systems were considered: aqueous suspensions of nanoparticles that solidify during the drying. Depending on the geometry involved, mechanical instabilities occur to release the mechanical stresses build-up. Such processes are governed by an energy minimization and foster cross-disciplinary areas specifically at the junction between Mechanics and Physics.

At the beginning of the 2000s, these works benefited from regular visits of Yves Couder at the FAST laboratory in the Université Paris Sud. It was a real opportunity and privilege to spend several hours with Yves to observe the formation of crack patterns under optical microscope, to search the proper conditions of growth and boundaries to form isotropic patterns, to reveal some details of directional growth of fractures, to add microscopic defects as nucleation centers to propagate fractures at will [8],... As the laboratory is bordered by a forest on the Plateau de Saclay, Yves usually left for a walk and came back with particular leaves to be observed under the microscope, and to reproduce similar patterns using drying fractures. As most studies initiated by Yves, elegance and simplicity are combined to powerful physical meaning. This gives a new dimension to works on mechanical instability induced by drying that were firstly initiated by Catherine Allain at the end of the 1990s [9, 10].

The present manuscript is articulated around both morphogenetic processes stated above. After a presentation of the topics related to morphogenesis, the manuscript aims to focus on the analogue experiments, their adaptability to reproduce patterns to explore specific properties of the media at a macroscopic scale, and the capacity to tune modelled systems in order to highlight the physical insights.

1.1. *Hierarchical crack pattern*

The veins of plant leaves exhibit a large variety of morphologies. By closely examining a leave, the network of veins provides various lengths and widths, and results in isotropic or anisotropic arrangements. In the most common nervation, called the dicotyledons, a main axial vein grows first. Then secondary veins are pinnately arranged along the middle vein. The multitude of resulting patterns provides an optimized network throughout their evolution. Numerical models showed that the network of veins provides the mechanical rigidity of the leave but this is not the single function of venation [11]. Indeed veins progressively canalise the flow which is physiologically of interest throughout its evolution and its lifetime. In particular, an essential characteristic of venation is dominated by the systematic reconnections, e.g. the merging of two veins to form a closed loop. Such reconnections are visible in the examples shown in Figure 1 [4].

The large variety of morphologies exhibited by the veins of plants was often thought to result from the growth in a concentration scalar field. The study initiated by Yves Couder shows that many characteristics of venation patterns correspond to what is expected from growth in a tensorial stress field. Numerous problems take place where structures grow in a diffusive scalar field [12]. They all result in branched tree-like patterns: viscous fingering, growth of a bacterial

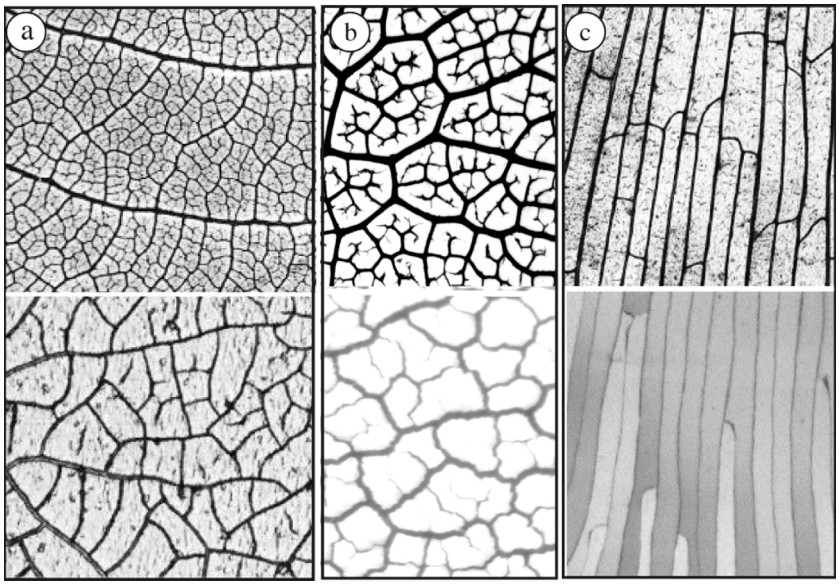

Figure 1. Patterns of veins in vegetal leaves and patterns of cracks in solids. (a–b) Comparison of the growth of veins and cracks in an isotropic medium. (a) *Top* – The higher-order veins are characteristic of a hierarchy which results from their successive order of formation. At each stage, they are connected in a polygonal pattern. *Bottom* – A pattern of cracks formed in a thin layer of dried gel. The resulting pattern exhibits a hierarchy of cracks delimiting adjacent domains. (b) *Top* – A detail of venation showing open-ended veinlets. *Bottom* – Crack pattern: at the end of the pattern formation, when most of the elastic energy has been released, some cracks stop growing without reconnecting and thus remain open-ended. (c) Comparison of the anisotropic growth of veins and cracks. *Top* – A detail of the venation in Lily of the valley. The pattern in this monocotyledon is formed of veins nearly parallel to each other. As the leaf narrows near its tip, the number of veins diminishes. When a vein stops growing, it reconnects perpendicularly to its nearest neighbour. *Bottom* – A pattern of cracks obtained in a dried gel layer having a constant thickness gradient along the vertical direction: the gradient build-up leads to a parallel array of cracks. Due to the wedge shape of the gel, some cracks stop growing. When a crack stops growing it connects perpendicularly to its neighbour (top of the image). (a) and (c): Adapted by permission from Springer-Verlag [4] (2002).

colony or diffusion-limited aggregation (DLA) produce branched patterns but avoid forming closed loops. A different class of patterns are formed in a tensorial field: the resulting networks are then dominated by reconnections. The structures produced by the propagation of cracks are the archetype of such patterns. In this aim, analogue experiments were investigated on crack formation whose similar pattern can reproduce venation in different configurations. In particular, the array of smaller veins of dicotyledons that forms when locally the leaf growth has become homogeneous and isotropic; the class of monocotyledon is formed of veins nearly parallel to each other (Figure 1c).

From this work different studies have been developed to understand the crack networks in materials consisted of a layer deposited on a substrate. This first section is devoted to the variety of crack patterns whose organization is governed by the minimization of the energy of the system.

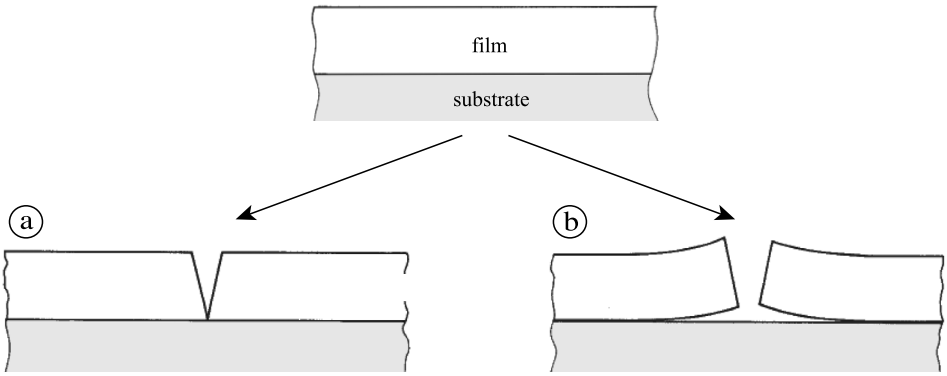

Figure 2. Two mechanical instabilities in a system film/substrate: (a) channeling crack in the thickness of the film, or (b) film/substrate separation causing delamination from an edge.

Analogue experiments have been performed in solid gels starting from a shallow container, filled by an aqueous dispersion of solid particles (silica beads whose mean diameter is ~10 nm). During water removal, the density of particles increases until the formation of a close-packed network that adheres to the glass plate (the substrate): a solid layer of approximately constant thickness is formed in the centre of the container avoiding the anisotropy due to large evaporation at the borders. Further evaporation induces pressure gradient in the poroelastic structure. As a result, the shrinkage at the free surface is frustrated by the adhesion on the substrate and leads to differential stress over the layer thickness. This process may cause the layer to crack releasing the mechanical stress.

More generally the crack patterns depend on the applied stress and the way the material can resist to this stress. Indeed, the resulting patterns are governed by a minimization of the energy of the system. It is stated that the elastic energy available for a crack growth requires the energy needed to create new crack surfaces in the solid [13]. Depending on the energies involved, a variety of mechanical instabilities can occur, whose two main modes are sketched in Figure 2: crack in the thickness of the film (channeling crack), interfacial crack emerging from an edge (delamination). Both processes are particularly considered in the following. A key parameter that controls the elastic energy stored in the layer is its thickness. Hence, below a critical thickness, h_c, the layers are crack-free as the elastic energy stored in the material is not sufficient to propagate cracks. Above h_c, the system fails when its strength, that is the maximum stress the material can withstand, is reached.

The organization of cracks in solid films are dominated by nucleation and propagation processes [14]. Depending on the material, the most frequent process can be either the nucleation of new cracks or the propagation of a pre-existing crack network. Since nucleation is more frequent for thin layers or inhomogeneous materials, propagation is predominant in thick and brittle materials. Indeed, for thin layers, the growth of the crack stops shortly after their initiation leading to junction cracks. The nucleation from defects can result in two-branched cracks in the same direction or star-like patterns with three-branched cracks at equal angles of 120° each other (Figure 3a). Since it costs less energy to create new surfaces at low thickness values, the number of branched cracks around a defect is expected to increase when the thickness decreases [15]. This is pointed out by the following simple considerations based on energy minimization. The energy needed to create new crack surface scales as $2n\Gamma\ell h$ (1), Γ being the surface energy of the newly-created interfaces, n being the number of the branched crack of length ℓ in a layer of thickness

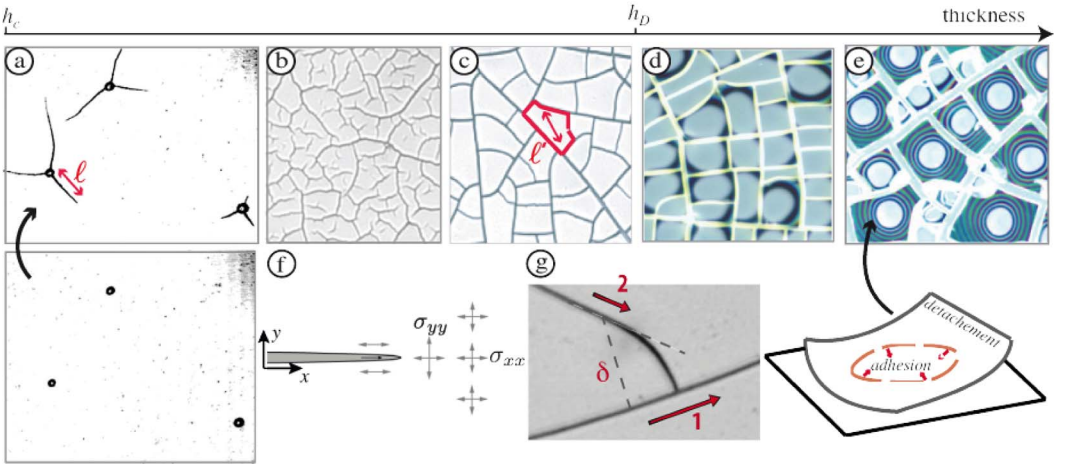

Figure 3. Crack networks as a function of the layer thickness (each image exhibit final crack patterns). (a) Star-like patterns with 3 branched cracks at 120° each other nucleated from nucleation sites (bubbles in the bottom image). (b) Broken network of cracks. (c) Close network of cracks limiting domains. (d, e) Partial delamination from the substrate confined at the edge of the domains (d); for thicker layers, inside a particular domain the circular optical interference fringes display an air gap and encircle an adhering region (bright area in (e)). (f) Sketch of the growth of cracks in an initially homogeneous stretched medium. (g) When a crack (2) propagates in the vicinity of a pre-existing crack (1), the crack path (2) is modified to take into account the stress release of (1).

h. In the presence of such a crack, the elastic energy in a cracked layer of thickness h changes by $\Delta U \sim \ell h^2 \bar{\sigma}^2/E$ (2), where ℓh^2 is the volume in which the stress relaxes, and $\bar{\sigma}$ the average stress in a volume element of lateral size ℓ. In the case of differential stress-induced by the drying, the main tensile stress, P, acts on the bottom surface. The volume-averaged tensile stress in the film, $\bar{\sigma}$, and P can be related using the fact that the average stress in a volume element can be related to an integral over the forces acting on its boundaries (in the case of wet particulate coatings $|P|$ can be viewed as the capillary pressure). Hence the average stress scales as: $\bar{\sigma} \propto P\ell/h$ (3) [16]. Combining both the surface (1) and the elastic (2) energies, taking into account the average stress (3), show that the number of branched crack, n, decreases when the film thickness, h, increases as: $n \propto \ell P^2/(\Gamma E)(\ell/h)^2$.

Contrarily, for slightly thicker layers, crack propagation is energetically more favourable than for thinner ones. The *zigzag* pathway is often associated with a difficult crack propagation. A typical broken network of cracks is shown in Figure 3b. For thicker layers, the crack merging is more frequently observed. Finally, a closed network is formed resulting in adjacent domains exhibiting a more or less regular size. The pattern exhibits angles between cracks at their junctions being mostly near 90° and 180°, as one would expect for T-junctions. Moreover, the averaged domain size, ℓ', increases with the layer thickness (Figure 3c). As previously mentioned, the cracks form when the energy cost of creating new surfaces at the sides of a domain is equal to the elastic energy released during the cracking. These energetical considerations write this time: $\ell' P^2 \ell'^2/(h^2 E) \propto \Gamma$. It result in the following scaling law valid for a particular range of thicknesses: $\ell' \propto h^{2/3}$ [16].

For still thicker layers the stored elastic strain energy generally overcomes the adhesion energy of the film attached to the substrate. As a result, another mode of cracking is energetically preferred: the interfacial cracking that propagates at the layer/substrate interface and results

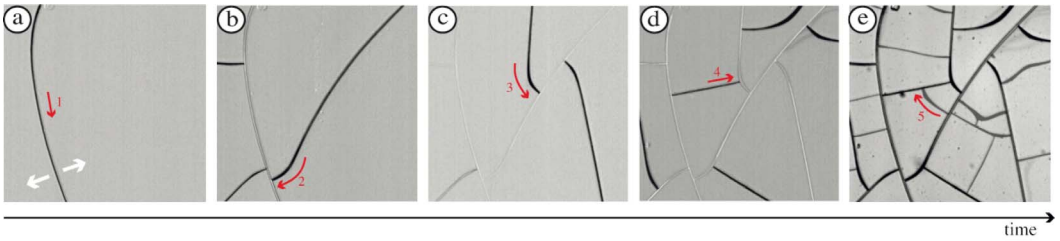

Figure 4. Hierarchical crack formation. Invasion of the plane of the layer by successive generations of cracks. From left to right: first, second, third and fourth order. In each image of the sequence a–d, the cracks of higher orders are highlighted in black; in each image the red arrows highlight one particular crack of a new generation. The final pattern is shown in (e).

in curling the domains. The interface crack starts generally propagating from the corners of a domain as a result of the stress concentration there [17]. The nucleation of the interface crack defines the final shape of the delaminated domain. The energy cost to create new surfaces competes with the elastic energy mainly due to the fold limiting the adhering region from the detached one that tends to be minimized [18]. Here again, the layer thickness controls the strain energy stored in the volume of the material and so the final pattern. The final pattern results in delamination that is either confined to the edges of each domain (Figure 3d) or causing each domain adhering by a single and preferentially circular region for thicker layers (Figure 3e).

Coming back to the case of plane-divided patterns prior to the delamination process, one specificity of the crack network shown in Figure 3b is presented in the following. Indeed, cracks invade the plane of a layer following well-defined rules of Physics as shown by the sequence in Figure 4 [5,6]. Generally, a crack pathway is formed by tensile stresses in the layer (sketched by the white dashes in Figure 4a). Once the crack is formed, the component of the stress normal to the crack path is released in its vicinity. Consequently, new boundary conditions are defined and will affect the pathway of further cracks. Indeed, when a future crack approaches the existing one, its path is changed due to the stress release of the first one. The new crack connects to its neighbor perpendicularly (Figure 4b). Hence, a progressive invasion of the plane of the layer takes place. At the final stage of the hierarchical cracking process, the history of the crack network formation can be approximately recovered. Indeed, the longer crack is generally the first to form, the second generation of cracks connect to the first one and so on...

Apart from the lengthscale associated with the crack spacing a quantitative aspect of a crack pattern is the number of sides and neighbours of a particular domain (see the histogram in Figure 5a). The theorem of Euler on topology states that the average number of neighbours in an extended network, hierarchical or not, must be six. In contrast to the geometrical hierarchy of a crack pattern, a two-dimensional soap separating the bubbles does not have any hierarchical structure (Figure 5b). The geometric structure of the last is given by reorganization phenomena: the lines corresponding to the films are arcs of circles and the angles at the vertices are adjusted to 120° following the laws of Plateau. Hence, the Physics of foams is largely governed by the enduring and symmetrical interaction of first neighbours. Such phenomenon is absent in the hierarchical crack pattern [5, 19].

Another similar pattern whose adjacent domains exhibits several sides and neighbours equal to 6 is the regular hexagonal tessellation formed by cooling shrinkage of sedimentary rocks [20]. Such a pattern is presented in Figure 5c: the cracks are formed simultaneously and appear as star-shaped connections. Contrarily to the hierarchical organization of a crack network in a

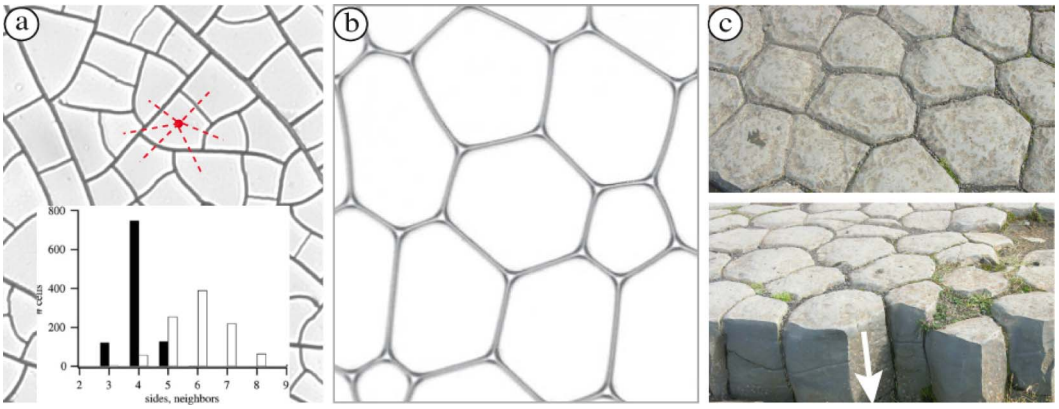

Figure 5. Hierarchy or not. (a) Network of cracks in a dried planar gel. The histogram shows the number of sides (black) and the number of neighbors (white) of 1000 domains in a ceramic crack pattern; as an example, the domain pointed out by the red dot has 6 neighbors (dashed lines) but 4 sides. (b) A six sided domain in foam. Reprinted from [19] "Hierarchical crack patterns: a comparison with two-dimensional soap foams", Copyright (2020), with permission from Elsevier. (c) Pattern of hexagonal tessellated pavement, Iceland (Courtesy of J.P. Hulin); the white dashed indicates the direction of cracks extension.

two-dimensional surface, the formation of a pattern of hexagonal tessellated pavement must be related to the cooling shrinkage in-depth in the material [21, 22].

2. Gastrulation

This section is devoted to another morphogenetic process involved in the mechanical evolution of embryos. During a particular stage called gastrulation, the embryo undergoes an invagination process. This mechanism appears to be a generic process that results in the precursor of the formation of the inner organs. The process was particularly studied in an archetype, that is the sea-urchin embryo, mainly for its geometrical simplicity. Indeed, the sea-urchin embryo exhibits a spherical shape typically small, ranging from about 3 cm to 10 cm in diameter [23]. Before gastrulation, the sea-urchin has a nearly spherical shell-like membrane that encloses a fluid-filled cavity: the blastocoele. The membrane is formed of a single layer of 1000 to 2000 cells: the blastoderm. During a first stage, a region of the membrane, called the vegetal plate, flattens while the cohesion of the cells in this region is reduced. Then a reversal of curvature of the membrane takes place, as a buckling process. During a second stage, the depressed region extends and forms a tube penetrating into the blastocoele (see the sketch in Figure 6a, b). This deformation is accompanied by movements of cells within the blastoderm from the external surface to the interior of the embryo. This process modifies locally the thickness and the mechanical properties of the membrane.

The similarity with an analogue experiment captures a stage of evolution of embryos without taking into account the movements of cells within the membrane. Different biological assumptions have been put forward to highlight and explain this process. It is not for us to discuss the validity of these hypotheses. The analogy particularly highlights that the second stage, e.g. the formation of an invaginated tube, could also be due to a continuation of a buckling process. This would only require that the shell exhibits inhomogeneous mechanical properties and that the cohesion of the shell be weaker in the region where the buckling occurs [7].

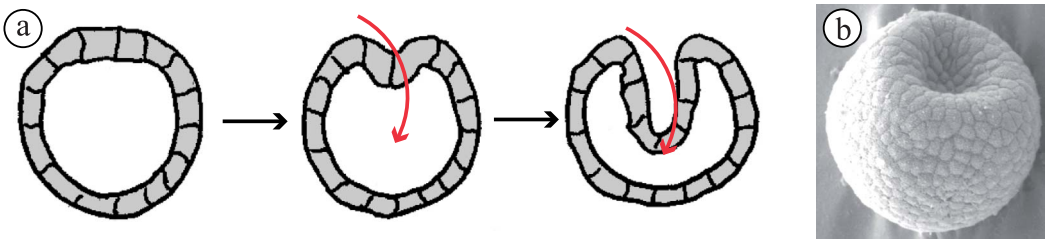

Figure 6. Sketch of the gastrulation in a Sea Urchin Embryo. During a first stage, a region of the membrane, called the vegetal plate, flattens and thickens while the cohesion of the cells in this region is reduced. This precursor of the deformation is caused by some movements of cells within the membrane. Then a reversal of curvature of the membrane takes place. The depressed region extends and invaginates. (b) Scanning electron micrograph of external surface of the early gastrula (Lytechinus variegatus, 500 µm in diameter) showing the reverse of curvature of the vegetal plate and the beginning of the invagination process into the blastocoele; courtesy of Morrill and Santos [23].

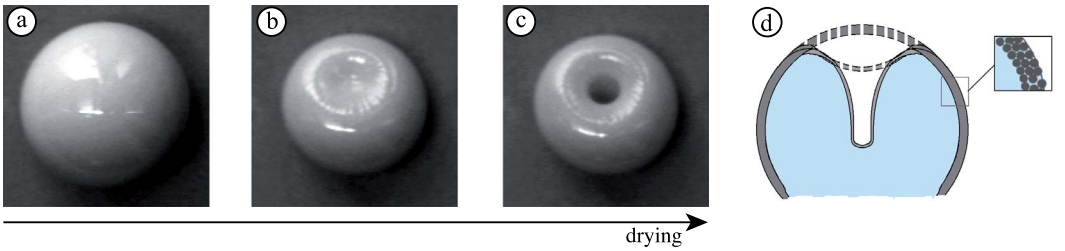

Figure 7. Deformation of a drying drop on a superhydrophobic substrate (top view); the drop is composed of a dispersion of nanoparticles (latex). After a nearly uniform shrinkage (a – meridian radius = 1.2 mm), a depression due to a local buckling takes place (b). The continuation of the buckling process results in a toroidal shape (c). (d) Sketch of the successive deformations in side view.

Such nearly spheroidal geometry is obtained by depositing a droplet of dispersion of nanoparticles on a superhydrophobic substrate. During the water removal, the drop firstly shrinks nearly isotropically as the non-volatile compounds are advected to the evaporation surface of the drop. This accumulation thus leads to the formation of a boundary layer, at the evaporation surface, through which the concentration changes. When the close packing of particles is reached, a porous skin behaves mechanically as an elastic shell enclosing a liquid phase. The formation of such a skin induced by the drying process depends on the physicochemical properties of the solution and well as the processes of diffusion and advection that govern the transport of particles in the dispersion [24, 25].

The morphological evolution of the shell-shaped membrane depends on the mechanical properties of the system. In particular, the more concentrated the dispersion is, the faster the porous thin skin will form. During later drying, the water continues flowing through the porous membrane allowing the drop to shrink as a result of the volume decrease (Figure 7a). The skin is capable of deformation due to the decrease in its inner volume. The successive stages of the drop deformation are shown in Figure 7a–c. The compression of the skin, e.g. in-plane displacement, leads to a length change that requires rapidly a great deal of energy in comparison with bending, e.g. out-of-plane displacement. This is a classical result: it corresponds to the

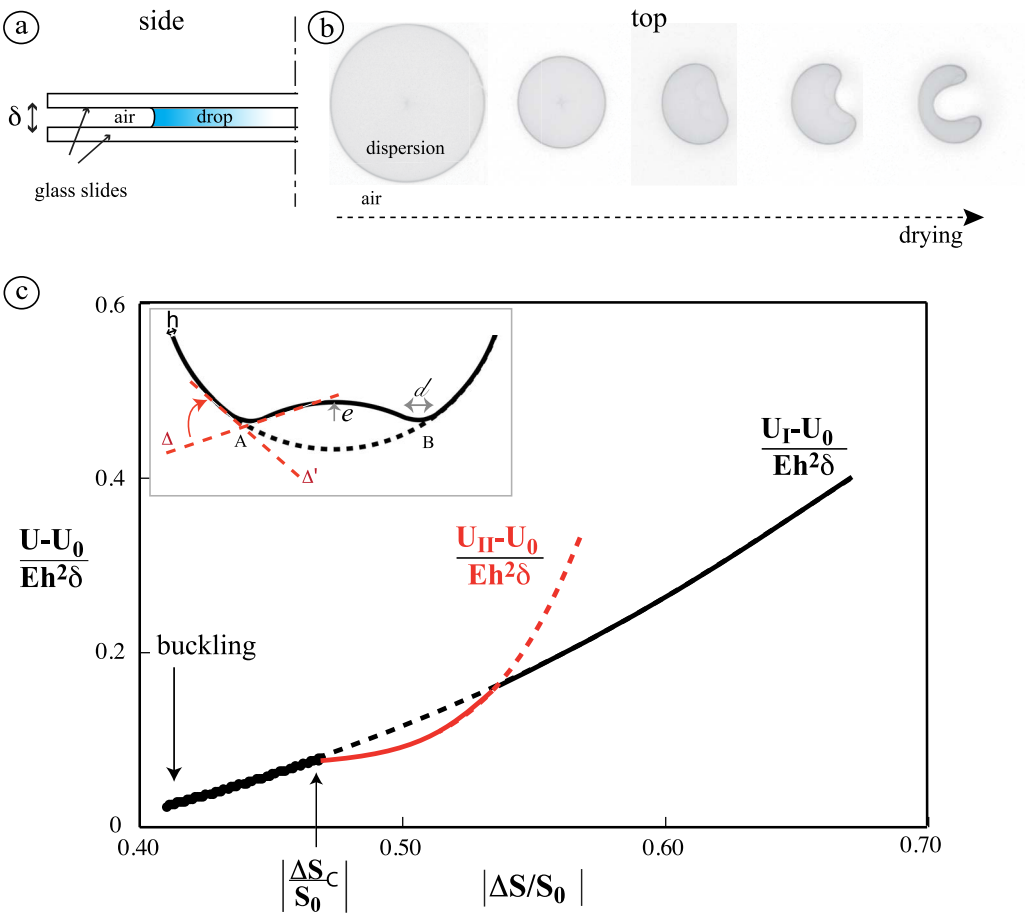

Figure 8. (a) Quasi-2D geometry: a droplet of solution is sandwiched between two circular glass slides in side view. (b) Deformation of a drop during the drying process in top view (initial drop diameter = 2 mm). (c) Dimensionless elastic energy of the shell at the periphery of the drop as a function of the relative surface variation $\Delta S/S_0$; U_0 is a reference energy term, U_I is the elastic energy whose main contribution comes from the creation of the folds A and B, and U_{II} is due to the folds A and B + the contribution of the change in length of the inverted part between A and B. Inset: ideal scheme of the depression formed by inversion of the circular cap between A and B the asymptotes Δ and Δ' limit the fold A. Adapted from [26].

first instability observed in the collapse of thin spherical shells [27]. In the presence of such a depression, extensional deformations are not energetically favourable and bending deformations preferentially take place. The depressed region then extends and invaginates inside the drop (Figure 7b, c). During this process, the mechanical behaviour of the membrane is locally modified resulting in inhomogeneity of the membrane. Indeed, the evaporation rate through the area of the convex surface decreases with decreasing curvature as a result of a quick saturation in water vapour in the curvature. The single depression at the top of the drop then deepens and forms an invaginating tube.

Moreover the evolution of the shell-shaped membrane can be investigated in confined geometry allowing us to precisely capture the second sage of the deformation [26]. In this way a

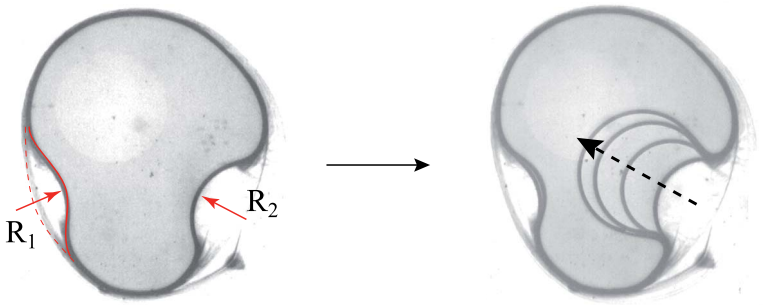

Figure 9. Drop exhibiting two depressions whose radii of curvature are R_1 and R_2 in the geometry depicted by Figure 8a. The superposition of images taken at successive times shows that only a single depression is continued by an invagination process.

drop was sandwiched between two parallel circular glass slides, providing a quasi-2D geometry (Figure 8a). The radial evaporation flux leads to the accumulation of non-volatile species at the liquid/air interface and results in the formation of skin at the drop surface. Simple energy considerations allow us to explain the continuation of the buckling process as highlighted by measurements deduced from the drop evolution (Figure 8b) [26]. During the depression growth, the elastic energy contains the main contribution coming from the creation of the folds *A* and *B*, denoted by configuration I, (inset in Figure 8c). Since the energy concentrated in the folds becomes enormous during the depression growth, another configuration, denoted by configuration II, is energetically more favourable. This is realized by freezing the folds *A* and *B*. Hence, the lateral size of the depression stops increasing and becomes constant. The elastic energy due to the fold only increases through the growth of the depression, e.g. apex *e* shown in inset of Figure 8c. The evolution of the drying drop is governed by an optimization of the energy of the system as highlighted by the plain lines in Figure 8c.

Finally, this quasi-2D geometry is a way to deal with the stability of such deformation in the case of a non-uniform membrane or when two depressions are initially nucleated. As the membrane is non-uniform, we can expect that only one depression can grow deeper inside the drop during water loss. When several depressions take place at the drop periphery (Figure 9), only one can last at the end of the invagination process. Such behaviour is analogous to viscous fingering development [1] where only one perturbation can grow in a diffusive field.

3. Conclusion

The manuscript reports some analogue experiments to understand spontaneous formations of patterns in Nature. These results attest of the reliability of laboratory experiments to highlight, isolate and then analyse mechanisms of interest acting in the self-organization of two distinct media: venation in leaves and deformation of embryos. Moreover, these results support the fact that morphogenetic processes are governed by energy minimization of the systems. One common element to these approaches is to describe out-of-equilibrium systems involving multi-component objects that strongly interact with each other at small scales via physicochemical surface interactions or mechanically through deformation. The main strength of this experimental modelling is based on tunable inter components forces and the diversity of physical properties emerging here during the drying process [28]. Thereafter, the study related to the crack network has been extended to different applications by relating the pattern and the matter, particularly the paintings cracks in artworks [29, 30].

Acknowledgements

I would like to thank some colleagues who have actively contributed to these studies: my long-time friend Mokhtar Adda-Bedia, Catherine Allain, Steffen Bohn, Stéphane Douady.

References

[1] Y. Couder, "Viscous Fingering in a Circular Geometry", in *Random Fluctuations and Pattern Growth: Experiments and Models* (H. E. Stanley, N. Ostrowsky, eds.), Nato Science Series E, Springer Netherlands, 1988, p. 75.
[2] E. Katifori, G. J. Szöllősi, M. O. Magnasco, "Damage and fluctuations induce loops in optimal transport networks", *Phys. Rev. Lett.* **104** (2010), 048704.
[3] Y. Bar-Sinai, J.-D. Julien, E. Sharon, S. Armon, N. Nakayama, M. Adda-Bedia, A. Boudaoud, "Mechanical stress induces remodeling of vascular networks in growing leaves", *PLoS Comput. Biol.* **12** (2016), no. 4, e1004819.
[4] Y. Couder, L. Pauchard, C. Allain, M. Adda-Bedia, S. Douady, "The leaf venation as formed in a tensorial field", *Eur. Phys. J. B* **28** (2002), p. 135-138.
[5] S. Bohn, L'empreinte de l'histoire dans la géométrie des réseaux bidimensionnels, PhD thesis, Université Paris 7 (2003).
[6] S. Bohn, L. Pauchard, Y. Couder, "Hierarchical crack pattern as formed by successive domain divisions. Part I: Temporal and geometrical hierarchy", *Phys. Rev. E* **71** (2005), 046214.
[7] L. Pauchard, Y. Couder, "Invagination during the collapse of an inhomogeneous spheroidal shell", *Europhys. Lett.* **66** (2004), no. 5, p. 667.
[8] L. Pauchard, M. Adda-Bedia, C. Allain, Y. Couder, "Morphologies resulting from the directional propagation of fractures", *Phys. Rev. E* **67** (2003), no. 2, 027103.
[9] C. Allain, L. Limat, "Regular patterns of cracks formed by directional drying of a collodial suspension", *Phys. Rev. Lett.* **74** (1995), p. 2981.
[10] L. Pauchard, F. Parisse, C. Allain, "Influence of salt content on crack patterns formed through colloidal suspension desiccation", *Phys. Rev. E* **59** (1999), no. 3, p. 3737.
[11] S. Bohn, B. Andreotti, S. Douady, J. Munzinger, Y. Couder, "Constitutive property of the local organization of leaf venation networks", *Phys. Rev. E* **65** (2002), 061914.
[12] Y. Couder, "Viscous fingering as an archetype for growth patterns", in *Perspectives in Fluid Dynamics* (G. K. Batchelor, H. K. Moffatt, M. G. Worster, eds.), Cambridge University Press, 2000, Ch. 2, p. 53104.
[13] A. Griffith, "The phenomena of rupture and flow in solids", *Phil. Trans. R. Soc. Lond. A* **221** (1921), p. 582-593.
[14] V. Lazarus, L. Pauchard, "From craquelures to spiral crack patterns: influence of layer thickness on the crack patterns induced by desiccation", *Soft Matter* **7** (2011), p. 2552-2559.
[15] A. Groisman, E. Kaplan, "An experimental study of cracking induced by desiccation", *Europhys. Lett.* **25** (1994), no. 6, p. 415-420.
[16] X. Ma, J. Lowensohn, J. Burton, "Universal scaling of polygonal desiccation crack patterns", *Phys. Rev. E* **99** (2019), article no. 012802.
[17] H. Yu, M. He, J. Hutchinson, "Edge effects in thin film delamination", *Acta Mater.* **49** (2001), p. 93-107.
[18] L. Pauchard, "Patterns caused by buckle-driven delamination in desiccated colloidal gels", *Europhys. Lett.* **74** (2006), no. 1, p. 188-194.
[19] S. Bohn, "Hierarchical crack patterns: a comparison with two-dimensional soap foams", *Colloids Surfaces A: Physicochem. Eng. Aspects* **263** (2004), p. 46-51.
[20] D. Branagan, H. Cairns, "Tessalated pavements in the Sydney region, New South Wales", *J. Proc. R. Soc. New South Wales* **126** (1993), p. 63.
[21] L. Goehring, L. Mahadevan, S. W. Morris, "Nonequilibrium scale selection mechanism for columnar jointing", *Proc. Natl Acad. Sci. USA* **106** (2009), no. 2, p. 387-392.
[22] G. Gauthier, V. Lazarus, L. Pauchard, "Shrinkage star-shaped cracks: Explaining the transition from 90 degrees to 120 degrees", *Europhys. Lett.* **89** (2010), p. 26002.
[23] J. B. Morrill, L. L. Santos, "A scanning electron micrographical overview of cellular and extracellular patterns during blastulation and gastrulation in the sea urchin, Lytechinus variegatus", in *The Cellular and Molecular Biology of Invertebrates Development* (R. H. Sawyer, R. M. Showman, eds.), University of South Carolina Press, Columbia, SC, 1985, p. 333.
[24] T. Okuzono, K. Ozawa, M. Doi, "Simple model of skin formation caused by solvent evaporation in polymer solutions", *Phys. Rev. Lett.* **97** (2006), p. 136103-136106.
[25] M. Léang, D. Lairez, F. Cousin, F. Giorgiutti-Dauphiné, L. Pauchard, L.-T. Lee, "Structuration of the surface layer during drying of colloidal dispersions", *Langmuir* **37** (2019), no. 7, p. 2692-2701.

[26] F. Boulogne, F. Giorgiutti-Dauphiné, L. Pauchard, "The buckling and invagination process during consolidation of colloidal droplets", *Soft Matter* **9** (2013), p. 750-757.
[27] R. L. Carlson, R. L. Sendelbeck, N. J. Hoff, "Experimental studies of the buckling of complete spherical shells", *Exp. Mech.* **7** (1967), p. 281-288.
[28] P. Bacchin, D. Brutin, A. Davaille, E. Di Giuseppe, X. D. Chen, I. Gergianakis, F. Giorgiutti-Dauphiné, L. Goehring, Y. Hallez, R. Heyd, R. Jeantet, C. Le Floch-Fouéré, M. Meireles, E. Mittelstaedt, C. Nicloux, L. Pauchard, M.-L. Saboungi, "Drying colloidal systems: Laboratory models for a wide range of applications", *Eur. Phys. J. E* **41** (2018), no. 8, p. 94.
[29] S. Lahlil, J. Xu, W. Li, "Influence of manufacturing parameters on the crackling process of ancient chinese glazed ceramics", *J. Cultural Heritage* **16** (2015), no. 4, p. 401-412.
[30] F. Giorgiutti-Dauphiné, L. Pauchard, "Painting cracks: A way to investigate the pictorial matter", *J. Appl. Phys.* **120** (2016), no. 6, 065107.